

## Asymmetric catalytic hydrogenations at micro-litre scale in a helicoidal single channel falling film micro-reactor

C. de Bellefon<sup>a,\*</sup>, T. Lamouille<sup>a</sup>, N. Pestre<sup>a</sup>, F. Bornette<sup>a</sup>,  
H. Pennemann<sup>b</sup>, F. Neumann<sup>b</sup>, V. Hessel<sup>b</sup>

<sup>a</sup> *Laboratoire Génie des Procédés Catalytiques, CNRS/ESCPE Lyon, F-69100 Villeurbanne, France*

<sup>b</sup> *Institut für Mikrotechnik Mainz, Carl-Zeiss-Strasse 18-20, D-55129 Mainz, Germany*

Available online 24 October 2005

### Abstract

A micro-structured single channel falling film is used for gas–liquid contacting. A small falling angle of 7.5° is used to ensure long residence time in the range 3–22 min, even with low viscosity solvents such as methanol. Using this device, a screening of molecular catalysts of the type rhodium/chiral diphosphines for the asymmetric hydrogenation of Methyl-Z-( $\alpha$ )-acetamidocinamate and similar substrates has been performed. The very small reacting volume of 14  $\mu$ l leads to an average inventory of Rh/test as low as 0.1  $\mu$ g. Comparisons with traditional batch experiments are provided.  
© 2005 Elsevier B.V. All rights reserved.

**Keywords:** Homogeneous catalysis; Catalyst screening; Kinetic; Micro-reactors; Asymmetric catalysis

The interest in conducting chemical reactions in micro-structured reactors (MSR) is enjoying a large interest [1–5]. While first experiments were motivated by the idea that physical phenomenon such as diffusion, momentum, mass and heat transfers are scale dependant, the chemical reaction, i.e. the intrinsic kinetics, is not. Thus, many catalytic reactions limited by heat and/or mass transfer in traditional equipments/reactors, have been conducted in or with the help of micro-structured components, mixers, heat exchangers, reactors... [1]. The ultimate hope was to design production units by scale-out of micro-structured components, mainly using staking/parallelization as the scale-out method. It was also recognized that micro-structured components, because of their low mass and thermal inertia, were able to offer short response time and/or for unsteady state periodic operations [6,7]. It is surprising that the idea to use micro-structured devices simply because of their very small reaction volume, i.e. the very low inventory of material required to gain some chemical information, has been exploited later [8]. Today, many reports describe the application of MSR as outstanding laboratory tools for e.g. screening applications [9,10], kinetics determination [11,12], process

data acquisition [13], for which no physical phenomenon are limiting in well design traditional reactors, but with the only concern to gain as much information as possible with as low reagent inventory as possible.

The use of MSR as laboratory tools for reactions involving one fluid phase is largely documented, e.g. for liquid phase organic synthesis or for gas–solid and liquid–solid catalysis. However, very few reports deal with reactions involving immiscible fluids such as gas–liquid or liquid–liquid catalysis [1]. This stems from difficulties to ensure appropriate multiphase contact and mixing for such multiphase systems in very small reaction volumes. Three gas–liquid reactor principles may be used for catalytic reactions:

- The first uses a dispersion of liquid droplets into a continuous gas phase. While, it is well adapted to very fast interfacial reactions, it is of restricted interest for the rather slow ( $>30$  s) gas–liquid catalytic reactions. Also the circulation of liquid droplets in an open air atmosphere has been reported [14], no demonstration of this principle for catalysis in micro-structured reactors has been published yet.
- The second depicts a dispersion of a gas in a liquid continuous phase. In such a design, the G–L mass transfer efficiency is mostly related to the size of the gas bubbles. While this principle looks very attractive, it is limited: (i) by

\* Corresponding author. Tel.: +33 4 72 43 17 54; fax: +33 4 72 43 16 73.

E-mail address: [cdb@lgpc.cpe.fr](mailto:cdb@lgpc.cpe.fr) (C. de Bellefon).

the need of high liquid velocities to create the shearing forces required for the generation of small gas bubbles and (ii) by coalescence that leads to large gas bubbles thus to lower mass transfer efficiency and, in micro-structures, to potential wetting problems. Furthermore, both high liquid rate and fast coalescence drive to residence times too short for homogeneous catalysis. Demonstration of this principle for micro-structured reactors has been published [12,15–19].

- The third consists in contacting a liquid film with a gas phase. The liquid phase is driven with gravity as in industrial falling film or trickle bed reactors. Reactors with micro-structured falling films, such as the falling film micro-reactor (FFMR) from IMM, have been proposed and operated but for rather short residence times [15,20]. An other type of film contactor has been proposed with horizontal positioning of the liquid film [10,21]. The pump driven liquid flow allows very flexible residence times [10].

One remaining question concerns the design of gas–liquid contactors offering both very low liquid hold-up ( $<100\ \mu\text{l}$ ) for analysis/screening purpose, ideal flow behavior and residence time compatible with slow reactions ( $30\ \text{min} > t_R > 30\ \text{s}$ ).

This report describes the design and use of a single channel helicoidal falling film micro-reactor. In a first section, the design, assembly and characterization of the micro-structured reactor is described, including study of residence times. In the second part, applications for the gas–liquid asymmetric hydrogenation of mainly Z-methylacetomido-cinnamate (mac) and some other similar substrates with rhodium chiral diphosphine complexes are demonstrated. Screening of transition metal molecular catalysts obtained by mixing a library of transition metal precursor with a library of chiral ligands, restricted screening of a class of substrate for a given reaction, screening of operating conditions, i.e. pressure, temperature etc are performed.

## 1. Micro-reactor design and operation

The design was based on previous works demonstrating high throughput screening or experimentation (HTS/HTE) with micro-structured components coupled to fast serial operations

using low-volume samples in a flowing medium, i.e. using pulse operation [8,9,12]. Continuous contacting can be achieved by guiding a pulse via a continuous liquid stream and gravity can be used to transport liquid films. An advantage of the latter concept is that it avoids spreading of the film, when guided along a plane or cylinder of suitable material, to generate large specific areas. This approach is known as falling film concept and represents a renowned gas/liquid contacting principle, as stated above. Using the falling film principle, the above mentioned reaction times of several minutes can be reached either (i) using vertical reaction channel plates of several 10 cm length exceeding even 1 m, which is neither practical nor a smart solution, (ii) decreasing the falling angle to lower the contribution of gravity to drive the liquid or (iii) both. Therefore, a new, more compact design based on a helical guiding of the liquid film and on a small falling angle was developed. The aim was, while significantly enlarging the falling film path, to orient the shape on minimizing the reactor outer dimensions, which, however, must be done at the expense of overall throughput. In addition, a low-cost fabrication technique was searched to achieve such complex design.

For first feasibility tests on quality of fabrication and capability of forming falling films, taper cone shaped devices were made by CNC turning as manufacturing technique using a lathe (Fig. 1).

First cuts through such devices revealed the need for improving structural quality, particularly considering reducing surface roughness (Fig. 2, left). This was achieved by changing the construction material, design and fabrication parameters. As a result, much better defined channel structures were finally obtained (Fig. 2, right).

Taper cone devices are easily amenable to inspection of the complete fluidic path. Both the empty channel surface and the liquid surface of the filled channel are accessible by white light interferometry (Wyko NT 2000). Using *n*-butanol as liquid flowing in micro-channels of  $100\ \mu\text{m} \times 300\ \mu\text{m}$  cross-section, a complete filling of the micro-channels without any flooding or undesired wetting of liquid at surfaces could be proven (Fig. 3).

In the new channel design, plateaus were set on both sides of the micro-channel (see Fig. 2, right and Fig. 4, right), and not

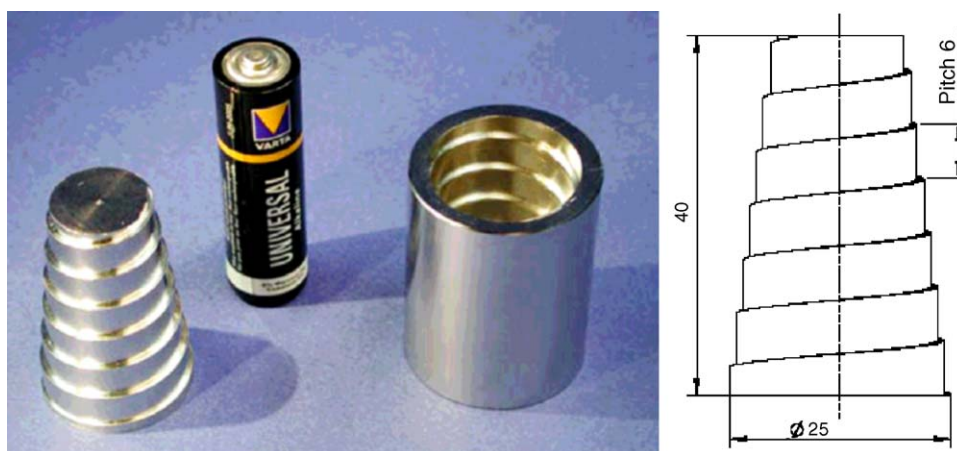


Fig. 1. Photograph of the tape cone shaped devices (left) and drawing of the helical guiding on outer and inner geometry (right).

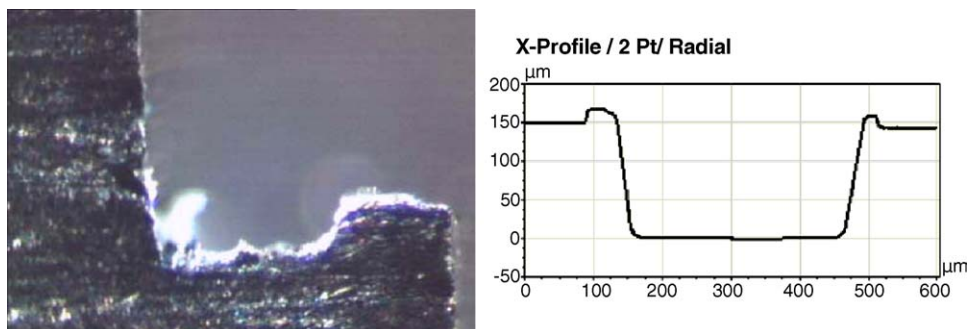


Fig. 2. Photograph of a cut of the engraved channel after initial manufacturing in aluminium (left). Optical profiling of another cut, made through a stainless steel device, yielding improved surface topography after changing manufacturing and design (right); please note: this design differs slightly from the right one.

only on one side as in previous designs (see Fig. 2, left). This helps to prevent undesired wetting of the taper cone/cylinder, which otherwise can result in a creeping of the film finally leading to blockage of movement by flushing out of the channel's volume. As drawback of the chosen taper cone design, limits with respect to fluidic path prolongation and respective increase in residence time have been identified. Thus, the fabrication approach was directed towards a cylindrical device with a helical flow path and its housing at last (Figs. 4 and 5).

The micro-structured cylinder is made of stainless steel (Fig. 6). The helical path was set to  $7.5^\circ$  which was considered low enough to allow large path prolongation on a given small reactor volume and high enough to avoid problems with liquid transport, e.g. due to stagnation as a result of too low velocity. The channel width and depth is set to 300 and 100  $\mu\text{m}$ , respectively. The diameter of the cylinder amounts to 24.3 mm. Three lengths of the helical path of 540, 1540 and 5390 mm (corresponding to a total device length of 70, 200 and 700 mm), residence times of 10, 30 and 105 min, respectively, are principally possible, provided that a continuous transport without evaporation can be achieved over such large times. The gas stream is guided through a cylindrical housing (Fig. 6).

The housing consists of a capped stainless steel tube (1.4571) with an inlet for the gas at the upper border, an upper cap with a liquid feed and a bottom cap with two outlets for gas and liquid (Fig. 7). For high pressure experiments the stainless steel housing can be used up to 50 bar at  $20^\circ\text{C}$ . Additionally, the stainless steel tube can be replaced with a transparent PMMA housing. This allows a visual inspection of the micro-

channels in the case of low-pressure experiments (up to 5 bar). Besides the micro-channel structuring, particular measures were undertaken to guarantee a reliable inlet and outlet of the liquid stream at the top and the bottom of the cylinder. For this special small inlet and outlet channels were fabricated. To monitor the butanol flow, a special optical set-up with illumination and fluorescence detection was used. The micro-structured cylinder (dismounted, i.e. not operated with housing) was filled using a piston pump at room temperature. At a certain time, a continuous stream of a fluorescent marker (such as fluorescein or fuchsin) in butanol or octanol replaced the pure solvent, thereby creating a stepfunction for the concentration (Fig. 7). This “step” was visible, at least for one or several passages around the cone. This way, the residence could be roughly determined.

The achieved residence times of both helical devices, the micro-structured taper cone and the cylinder, are listed in Table 1. It can be seen that the residence time of the new devices are much higher (about factor 50) in comparison to the standard falling film micro-reactor. Depending on the physical properties (viscosity) of the solvent, residence times from 3 min for methanol up to 22 min for octanol could be determined. The compactness, or smartness, is evident when normalizing micro-channel length by the long axis of the device (total device length) or the total device volume. These ratios of compactness are increased by more than an order of magnitude.

The study of residence time distribution have led to the determination of Peclet numbers in the range 58–74 which drive to the conclusion that a plug flow behavior can be ascribed to the helicoidal micro-channel falling film reactor.

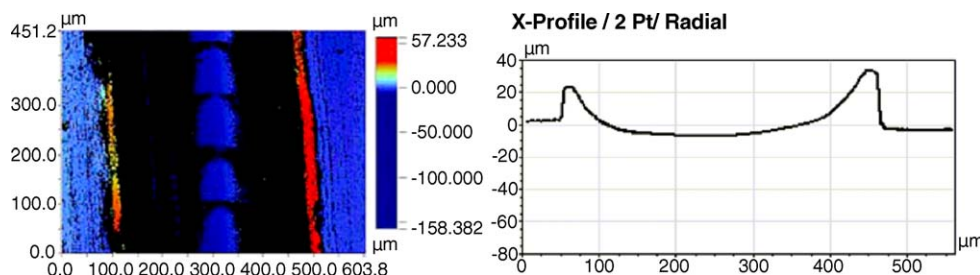


Fig. 3. Optical profiling of the liquid falling film in a helical guided micro-channel. Colour encoded image for depth profiles, showing in addition the pulsation of the pumps (left). Corresponding surface topography yielded from data of the left image (right).

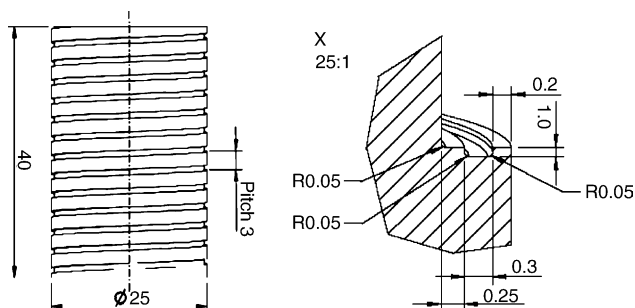


Fig. 4. CAD drawing of one of different design proposals for the new helical falling film micro-reactor. The design proposals differ in slope, respectively path length, and detailed shape of the micro-channel, which was regarded to be crucial for proper filling and flow of the liquid film.

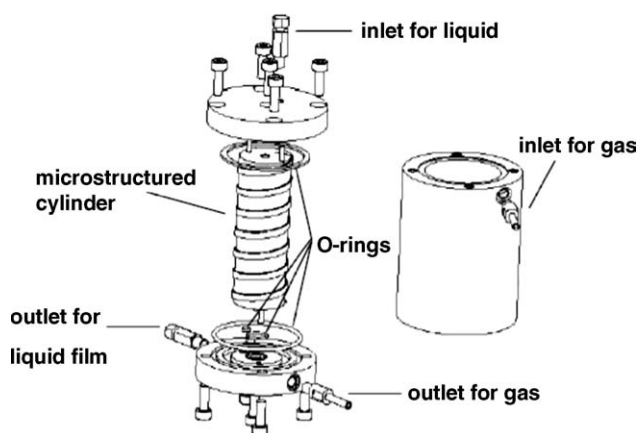


Fig. 5. CAD drawing showing the principle of assembly and guiding of gas and liquid flows.

## 2. Experimental

### 2.1. Chemicals

All experiments were carried out under nitrogen or argon. The reagents  $[\text{Rh}(\text{COD})_2]\text{BF}_4$  and the chiral diphosphines were supplied by Strem and used as received. The methanol (Aldrich) was degassed prior to use. Yields and conversion were determined quantitatively by gas-chromatography analysis.

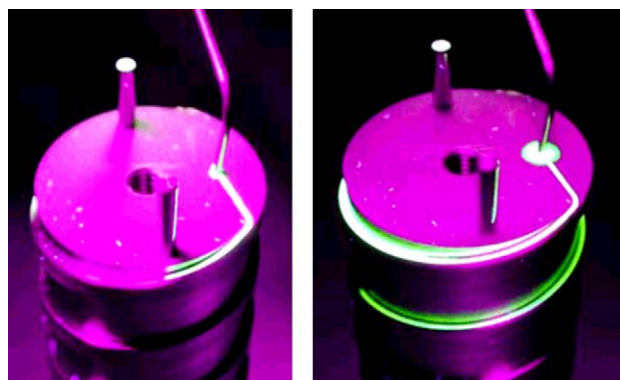


Fig. 7. Photographs showing the liquid distributor (left) and illustrating the capillary guiding of the liquid in the channel. Injection of a fluorescent tracer have also been used for determination of the residence time of the helical falling film micro-reactor.

### 2.2. Experimental set-up

The set-up used for gas–liquid operations is described in Scheme 1. The grey arrows indicates the flow movement during the refilling of the syringe and the black arrows the direction of the liquid while performing catalytic tests. The set-up includes the following equipment—A: liquid reservoir (MeOH); B: liquid syringe pump, C: injection valve equipped with a 20  $\mu\text{l}$  injection loop; D: gas flow-meter; E: helicoidal contactor; F: back-pressure regulation valve.

The dimensions of the micro-channel used in this tests are 509 mm length, 300  $\mu\text{m}$  width and 100  $\mu\text{m}$  depth which provides a total geometrical volume assuming a full flat-filling of the channel, of 15.3  $\mu\text{l}$ . The operating pressure is 1 bar since a more sophisticated back-pressure regulation valve would have been required to operate at higher pressure.

### 2.3. Catalysts preparation and asymmetric hydrogenations

A solution of metal precursor  $[\text{Rh}(\text{COD})]\text{BF}_4$  (0.0012  $\text{mol l}^{-1}$ ) in MeOH (3.7 ml) was added to a Schlenk tube containing the exact mass of the diphosphine to adjust the ratio metal:ligand (1:1) and the mixture is left for ca. 15 min under stirring at room temperature (28  $^{\circ}\text{C}$ ). A solution of Z-methylacetamido-cinamate(mac) (0.55 ml, 0.8  $\text{mol l}^{-1}$ ) is then



Fig. 6. New helical falling film micro-reactor with an extended path length of 540 mm.



Table 1

Comparison on scales and normalized scales and residence time, which is related to length scale, for three types of falling film micro-reactors

	Micro-channel length (mm)	Total device length (mm)	Micro-channel length/total device length (–)	Micro-channel length/total device volume (mm <sup>–2</sup> )	Residence time (min)
Standard FFMR <sup>a</sup>	66.4	120	0.55	0.021	Water/methanol: 0.2
Taper cone helical FFMR	440	50	8.8	0.350	Butanol: 9
Cylindrical helical FFMR	540	80	6.8	0.255	Methanol: 3.1
					Butanol: 12.7
					Octanol: 22

<sup>a</sup> See refs. [15] and [20].

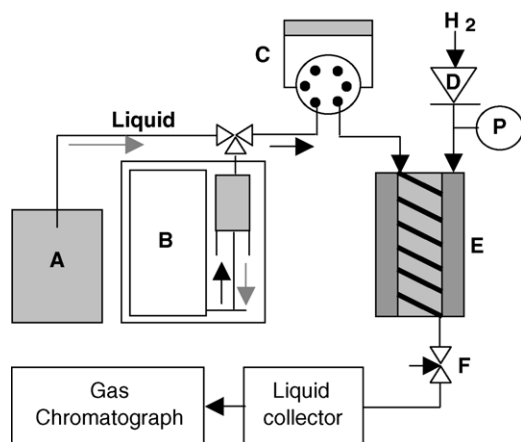
added. The total volume is 4.25 ml and the final concentration is 0.001 mol l<sup>–1</sup> for the catalyst and 0.1 mol l<sup>–1</sup> for the substrate mac. The so prepared solution was charged in the 20 µl loop of the Rheodyne (7725) injection valve. This valve is connected to a syringe pump (Bioblock A-99) that ensures a constant MeOH flow rate. The hydrogen flow rate is also kept constant with a mass flow-meter. After injection, the reacting pulse is drawn into the helicoidal micro-contactor and collected for 5 min in a 2 cm<sup>3</sup> vials at the outlet of the micro-reactor. Samples were analysed by gas chromatography on an HP-6890 apparatus equipped with a Chirasilval column (25 m, 0.16 µm, *d* = 0.25 mm, 6.5 cm<sup>3</sup>/min He, FID detector, split injection mode, 1 µl, 165 °C, 12 min).

Unless otherwise stated, the standard operating conditions are: MeOH flow rate: 0.707 cm<sup>3</sup> h<sup>–1</sup>, hydrogen flow rate: 5 scc min<sup>–1</sup>, [substrate]: 0.1 M, [Rh]: 0.001 M, injection loop: 20 µl, total pressure 0.1 MPa. The temperature may vary between 25 and 35 °C and is measured.

### 3. Results and discussion

The asymmetric hydrogenation of the pro-chiral substrate methylacetamidocynamate catalysed by rhodium diphosphine complexes has been investigated (Scheme 2) [22].

This class of reaction is of importance for the life products industry and has been the topic of the 2002 Nobel award. The aim was to demonstrate the use of the helicoidal falling film micro-reactor for the screening of catalysis.



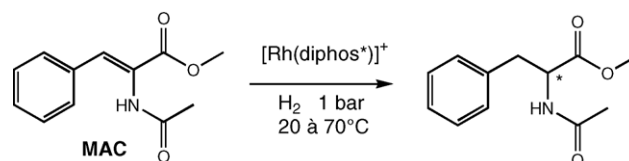
Scheme 1.

#### 3.1. Screening of catalysts and ligands

Both the molecular catalyst and the substrate mac are injected as a mixture in the organic solvent. Up to 17 chiral phosphines have been evaluated (Table 2). These are mostly diphosphines (P–P) ligands but some are nitrogen containing P–N ligands other are chiral mono-phosphines. This library is available from commercial resources. The rhodium complexes were prepared as stock solutions by mixing the [Rh(COD)<sub>2</sub>]BF<sub>4</sub> precursor and the diphosphine using Schlenk techniques with the exception of the commercially available Rh/Binap catalysts.

Because, by design, the test is limited both to rather short reaction time (3 min) and to low pressure close to ambient conditions, only those active catalysts display significant data. However, the criteria of activity is one of the most popular in the field of catalyst screening and the micro-device used here will provide information on the reactivity scale of the catalysts screened. The Diop ligand (entry 11) is the most active under the operating conditions of the test. The (*R,S*)Cy-Cy-Josiphos ligand (entry 15) is almost as good as the Diop ligand and provides a better enantioselectivity (75%). The latter ligand belongs to the class of the Josiphos type diphosphines (entry 12–14) but is clearly the most active of this family (88% conversion). It is interesting to note the inversion of the configuration of the main product between the two Josiphos of entries 13 (product *R*) and 14 (product *S*) having the same absolute configuration (*R,S*). Also of interest are the results for the (*R,R*)-Me-Duphos ligand (entry 3) which gives a very high enantioselectivity of >99.9% while displaying a fairly good activity (26% conversion). Again, a strong change is observed with the ethyl substituted analogue (*R,R*)-Et-Duphos (entry 2) which is not active.

The reproducibility of the data obtained has been checked with the Rh/Diop catalytic system, which is one of the fastest catalysed G/L asymmetric hydrogenation. Over five tests, the



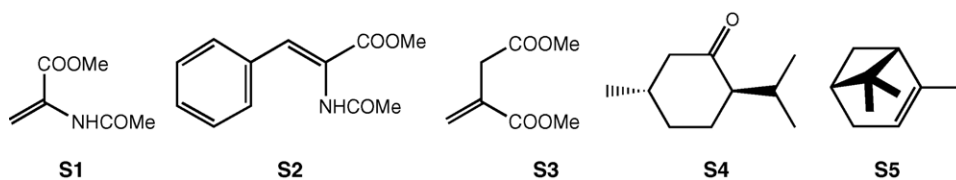
Scheme 2.

Table 2

Screening of 17 chiral phosphine ligands for the hydrogenation of Z-methylacetamidocinamate (mac) in the helicoidal micro-reactor

Entry	Ligand/catalysts	<i>T</i> (°C)	Conv (%)	ee (%)	Ligand (μg)
1	S-NMDPP	30.3	<1	13	7.13
2	( <i>R,R</i> )-Et-Duphos	30.1	1.6	>99	7.97
3	( <i>R,R</i> )-Me-Duphos	30.0	26	>99	6.74
4	( <i>R,R</i> )-Et-BPE	31.5	0	–	6.92
5	( <i>R,R</i> )-Me-BPE	31.4	1	84.6	5.68
6	( <i>R,R</i> )-Norphos	31.5	<1	–	10.18
7	( <i>S,S</i> )-Chiraphos	31.5	0	–	9.38
8	( <i>R</i> )-Prophos	31.5	<1	–	9.07
9	( <i>R</i> )-Trost ligand	27.5	0	–	15.20
10	( <i>R</i> )-Quinap	27.4	0	–	9.67
11	( <i>R,R</i> )Diop	33.5	94	63.5	10.97
12	( <i>R,S</i> )Josiphos	33.5	26.5	86.2	13.08
13	( <i>R,S</i> )- <i>t</i> -Bu-P-Josiphos	33.5	3	48.6	11.93
14	( <i>R,S</i> )Pcy-Josiphos	33.5	3.7	–7.6	13.08
15	( <i>R,S</i> )cy-cy-Josiphos	33.5	88.1	75.1	13.35
16	( <i>R</i> )-Binap	35	<1	23.7	12.45
17	( <i>R</i> )-[Rh(Binap)COD]BF <sub>4</sub>	35	<1	–	12.45
18	( <i>S,S</i> )-BPPM	35	22.5	91	11.07

Rh inventory per test 8.12 μg (20 nmol), ligand inventory per test: 22 nmol, reaction time: 3 min. Other operating conditions see Section 2. For comparison with literature data, see ref. [10].



Scheme 3.

mean deviation was 2% for conversions and less than 1% for the enantiomeric excess (ee) which proved the reliability of this new micro-device.

### 3.2. Screening of different substrates using the Diop chiral diphosphine

The gas–liquid micro-devices can also be used for the screening of different substrates using on catalyst. The catalyst precursor complex [Rh(COD)Diop]BF<sub>4</sub> have been used for the screening of five substrates containing pro-chiral C=C double bond (Scheme 3). Results are shown in Fig. 8.

S1 is methylacetamidoacrylate, S2 is Z-α-methylacetamidocinamate, S3 is dimethylitaconate, S4 is methone, S5 is α-pinene (1*R* + 1*S* enantiomers).

These results are in agreement with the general trends reported for asymmetric hydrogenations: Activated C=C such as acetamido derivatives S1 and S2 are more reactive [22]. The less sterically hindered substrate S1 is the most reactive. Unsubstituted and sterically hindered substrates such as S4 are not very reactive and reduction of C=O bonds such as in S5 are more difficult. Enantiomeric excess data (ee) are not predictable but are in good agreement with reported data on similar substrates (note here that the 100% ee at 1.5% conversion reported for S5 is likely to be lower at higher conversions) [10,22].

### 3.3. Extended studies on catalyst inventory

This section is related to the criteria of sample inventory. A series of experiments was performed to demonstrate the ability of the test to operate within a broad range of catalyst concentrations corresponding to a wide range of catalyst inventory. Thus tests with the standard catalyst precursor complex [Rh(COD)Diop]BF<sub>4</sub> have been performed over the

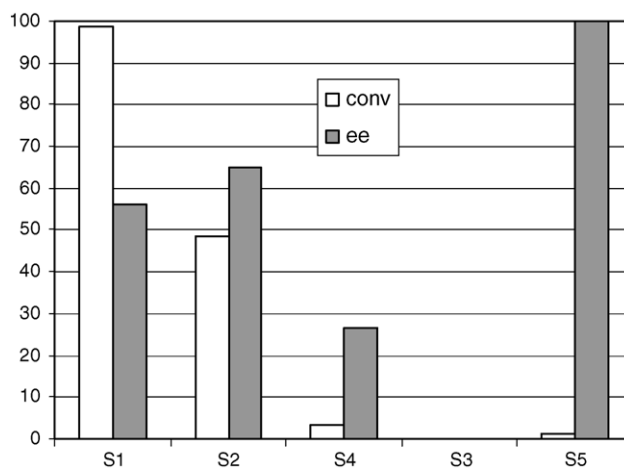


Fig. 8. Screening of 5 substrates. Reaction time: 8 min, 35 °C.

range of concentration  $10^{-5}$  to  $10^{-3}$  kmol m $^{-3}$  that is generally used in asymmetric hydrogenations with Rh complexes.

These results drive to three very important observations: (i) the observed linear dependence of the rate, which is represented here by the conversion at a given reaction time, with the catalyst concentration is in agreement with the general behaviour of molecular transition metal catalysts, (ii) the catalyst concentration does not affect the enantioselectivity, which was also expected for this type of catalysis, (iii) the system allows to work with very low catalyst concentrations down to  $5 \times 10^{-5}$  kmol m $^{-3}$  which translates into very small catalyst inventory, down to 0.08  $\mu$ g of Rh and ca. 0.2  $\mu$ g of ligands (depending on the ligands molecular weight), these results being obtained in a reproducible and quantitative way.

### 3.4. Investigation of catalyst preparation

In order to further explore the multiple capabilities of the gas–liquid micro-reactors, the helicoidal micro-falling film reactor was used for the investigation of molecular catalysts preparation. Thus, many parameters which are known to influence the catalyst preparation have been reviewed and screened using this micro-device. With this aim, a standard catalyst, the rhodium complex [Rh(COD)Diop]BF $_4$  known to afford reproducible results in conventional equipments, was selected.

From the literature, the preparation of catalysts of the type [Rh(diene)diphos] $^+X^-$  (diene = COD ou NBD) and  $X = BF_4$  or  $PF_6$ ) appears quite straightforward [22]. Two well known preparations are reported, the addition of the organometallic precursor [Rh $_2(\mu Cl)_2(COD)_2$ ] to the diphosphine ligand and metathesis of the chloride anion with  $X^-$  (use of TlPF $_6$ ) and the substitution of one of the diene COD ligands in the precursor [Rh(COD) $_2$ ]BF $_4$  with the diphosphine ligand. Once prepared, the catalyst solution can be either used as a stock solution or further worked-up to give a solid material via crystallisation or precipitation.

Note that in some instance, it is recommended to activate the catalyst under hydrogen before use. This activation procedure is known to reduce the remaining diene ligand in order to offer free coordination sites to the incoming substrate. Some reports describe an “induction period” while operating the hydrogenation reaction without the pre-treatment (activation) [22]. Last but not least, the nature of both the diene and the diphosphine ligand is of importance. For example, the size of the chelate ring formed by complexation of the disphosine has an influence on the catalyst activity. It is known that five member metallo cycles are less active than seven member ones. From this study, it can be seen that the efficiency of the molecular catalysts depends on numerous qualitative and quantitative parameters during the catalyst preparation and may deserve an multi-parameters optimisation procedure.

First, the stability of two identical stock solutions of our target catalyst precursor [Rh(COD) $_2$ ]BF $_4$  and that of two stock solutions of the diphosphine ligand Diop have been evaluated. From these stock solutions, 4 (2  $\times$  2) in situ prepared catalysts can be tested. These catalysts should, in principle, be identical

Table 3  
Stability of stock solution of catalyst preparation

Entry	Catalyst	Conv (%)	ee (%)
1	A	11.7	62.0
2	B	39.9	63.4
3	C	43.6	65.5
4	D	40.2	63.3
5	D	32.9	63.4
6	D	32.7	63.7

since the concentration (0.001 kmol m $^{-3}$ ), solvent etc are the same. The results using the standard reaction (Scheme 2) are given in Table 3.

These results show that the reproducibility of the preparation is not too bad, only catalyst A displaying a conversion number far too low while catalysts B to D when freshly prepared and used, provide conversions in the range 40–44%, i.e. within experimental errors. Indeed, the stock solution of catalyst A decomposes as revealed by the characteristic dark colour. Entries 4–6 reveal a phenomenon related to catalyst aging (after 1 day storage) leading to a slightly less active catalyst. The selectivity numbers ee are very similar as expected. The information concerning the catalyst activation and aging was of tremendous help to apply a standard work-up procedure for the efficient storage of catalysts, catalyst precursors and ligands stock solutions (Fig. 9).

Second, the influence of the aging time on the activity (i.e. the conversion numbers) has been studied considering two main parameters: (i) the influence of the reaction time when mixing the catalyst precursor with the ligand (Fig. 10) and (ii) the influence of the contact time upon addition of the substrate and before reaction with hydrogen (Fig. 11).

These results clearly indicate that the aging time for the catalyst solution of ca. >1 h is required in order to reach the best and stable conversion numbers (ca. 40%) similar to those found

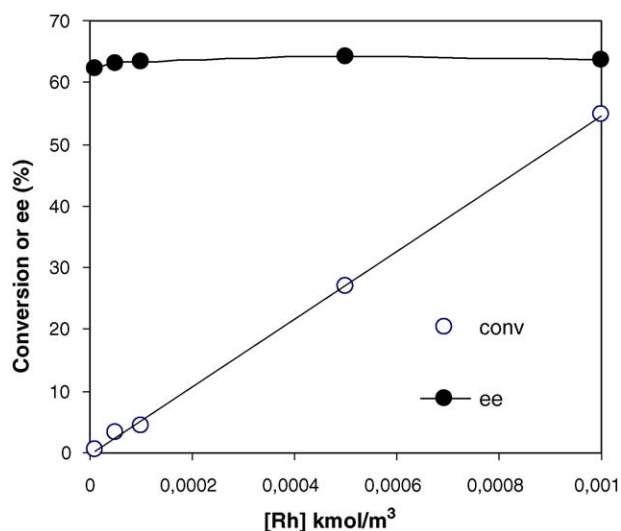


Fig. 9. Influence of the catalyst concentration on the conversion and enantiomeric excess. Operating conditions: methanol flow rate 0.398 cm $^3$  h $^{-1}$ . Other conditions: see Section 2.

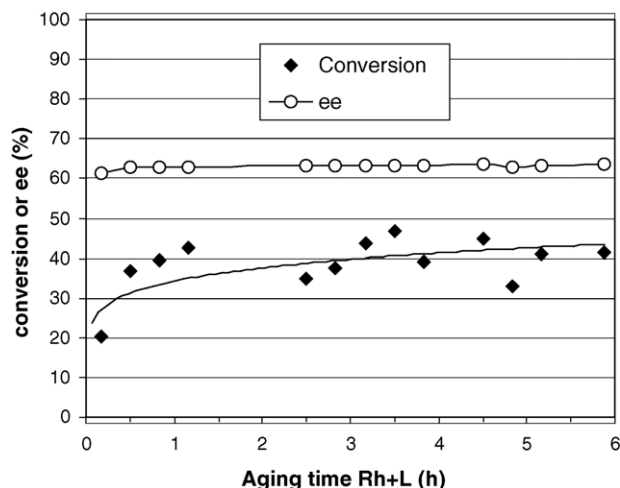


Fig. 10. Influence of increasing the aging time when mixing the rhodium precursor and the ligand prior to reaction.

in the table above. The enantioselectivity is not influenced by the aging time, ee lying in the range 61% after 10 min aging to 63% after 70 min.

The influence of aging time after addition of the substrate and before reaction with hydrogen for a catalyst that has been aged in the first step Rh + L for 10, 30 and 50 min, respectively, i.e. corresponding to the three first point in the figure above, is depicted below (Fig. 11).

For the sake of clarity, the enantioselectivity is not shown in the figure since it is constant (within 60–64%) irrespectively of the aging time. The conversions are all in the range 35–45% which could be considered as the average value (Table 3) except for the catalyst having been aged in the Rh + L procedure for only 10 min. A very important and clear conclusion is deduced on the fact that addition of the substrate has no influence on the catalyst performances. This demonstrate that the procedure is not biased by in situ mixing of a stock solution of the catalyst

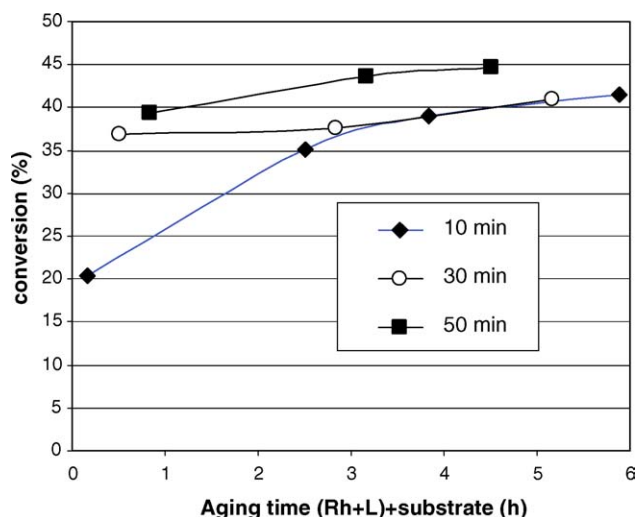


Fig. 11. Influence of increasing the aging time upon addition of the substrate to solutions of the rhodium precursor and the ligand prior to reaction.

with a stock solution of the substrate before reaction in the micro-tests.

### 3.5. Comparison with traditional reactors

The asymmetric hydrogenation of the pro-chiral substrate methylacetamidocynamate catalysed by the two rhodium diphosphine complexes Rh/Josiphos and Rh/Diop has been investigated in three different reactors. Reactor 1 consists of a circular arrangement of 12 screw-capped gas-tied glass tubes of ca. 20 cm<sup>3</sup> equipped with magnetic stirring and rods. This equipment is called “Caroussel” (Radleys Discovery Technologies) and is very popular as a top-bench equipment for parallel operations. Reactor 2 is a 25 cm<sup>3</sup> pressure reactor equipped with a turbine and baffles (Series 4590 from Parr Instruments). Reactor 3 is the single channel falling film micro-reactor. Such a comparison is of importance since many chemists tend to use both type (reactors 1 and 2) of equipments.

The experimental conditions used are: residence time 3 min. Pressure 0.1 MPa, 27–34 ± 0.1 °C. The catalysts are prepared as stock solutions from the precursor [Rh(COD)<sub>2</sub>]BF<sub>4</sub> and the corresponding diphosphine. The enantioselectivity were roughly the same in all reactors, in the range 80–90% and 62–65% for the Rh/Josiphos and Rh/Diop catalysts, respectively. However, the conversion numbers are very different (Fig. 12). Thus for a given residence time, i.e. reaction time, the batch reactor and the micro-falling film are performing much better than reactor 1 (Caroussel). The longer residence time required to achieve a given conversion (fixed at 9% for the *R,S*-Josiphos/Rh catalyst and at 46% for the Rh/Diop catalyst) with the parallel “Caroussel” reactor likely indicates under mass transfer regime (Fig. 12).

Mass transfer coefficients in the range  $k_1a = 1\text{--}2\text{ s}^{-1}$  are currently reached in small batch reactors [23]. Rather low mass transfer coefficient of ca. 0.01 s<sup>-1</sup> were measured in the Caroussel reactor [24]. In view of the conversion numbers (Fig. 12), the mass transfer coefficient in the single channel micro-falling film reactor should lie between these extreme values. Further characterisation of the mass transfer capabilities

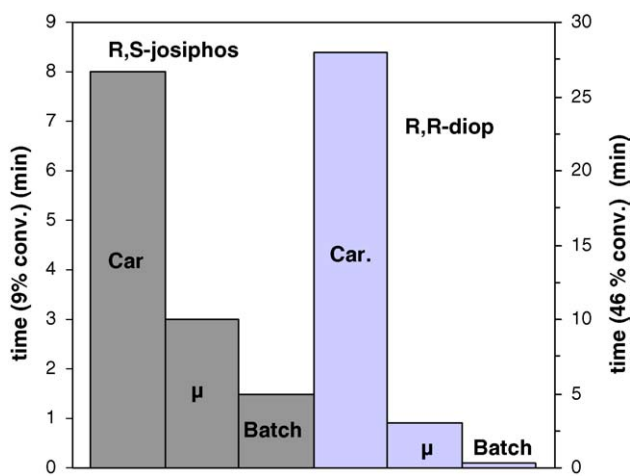


Fig. 12. Comparison of reactors with the most active catalysts Rh/Josiphos and Rh/Diop. The abbreviations car., μ and batch stand for reactor 2, 3 and 1, respectively.



cannot be performed since detailed kinetics are not available for the test reactions used in this work. Yet, since the enantioselectivity is not too much dependent on the gas–liquid mass transfer for these two catalysts, the effectiveness of the single-channel micro-reactor for the screening of gas–liquid reaction with very low inventory of material is demonstrated.

#### 4. Conclusion

The purpose of this work was to design, built and operate a micro-structured reactor adapted to the investigation of gas–liquid reaction and requiring a very low inventory of material per test. A single channel falling film micro-reactor (SCFFMR) displaying a liquid reaction volume as low as ca. 15  $\mu\text{l}$  has been fabricated and characterized. Asymmetric hydrogenations has been performed using the SCFFMR. Very reproducible results can be gained. The effectiveness of the SCFFMR has been proved for diverse applications currently performed in asymmetric catalysis such as screening of catalysts, ligands and substrates and also for catalyst aging and stability evaluation. Comparison with other traditional reactors reveals that the gas–liquid mass transfer coefficient might not be as good as in well behaved bench top pressure reactors but much larger than Schlenk like reactors. Furthermore, it has been demonstrated that very small changes in the chiral ligands (Me versus Et, etc. . .) leading to tremendous impact on activities and enantioselectivity, a well known but still unexplained phenomenon in asymmetric catalysis, can be accurately identified with an inventory as low as 0.2–13  $\mu\text{g}$  of the very expensive chiral ligands (ca. 300–1000 €/g) involved.

#### Acknowledgements

Funding from the European Commission (GRD-2000-256262), the CNRS and the Ecole Supérieure de Chimie Physique Electronique de Lyon is acknowledged.

#### References

- [1] V. Hessel, S. Hardt, H. Löwe, *Chemical Micro-process Engineering: Fundamentals*, Wiley-VCH, Weinheim, 2004.
- [2] P.D.I. Fletcher, S.J. Haswell, E. Pombo-Villar, B.H. Warrington, P. Watts, S.Y.F. Wong, H. Zhang, *Micro-reactors: principles and applications in organic synthesis*, Tetrahedron 58 (2002) 4735.
- [3] A. Graviolidis, P. Angeli, E. Cao, K.K. Yeong, Y.S.S. Wan, *Technology and applications of micro-engineered reactors*, Chem. Eng. Res. Des. 80 (2002) 3.
- [4] K. Jähnisch, V. Hessel, H. Löwe, M. Baerns, *Chemistry in micro-structured reactors*, Angew. Chem. Int. Ed. 43 (2004) 406.
- [5] K.F. Jensen, *Micro-reaction engineering—is small better?* Chem. Eng. Sci. 56 (2001) 293–303.
- [6] E.V. Rebrov, S.A. Duinkerke, M.H.J.M. de Croon, J.C. Schouten, *Optimization of heat transfer characteristics, flow distribution, and reaction processing for a micro-structured reactor/heat-exchanger for optimal performance in platinum catalyzed ammonia oxidation*, Chem. Eng. J. 93 (2003) 201–216 (and references cited therein).
- [7] A. Rouge, B. Spoetzi, K. Gebauer, R. Schenk, A. Renken, *Micro-channel reactors for fast periodic operation: the catalytic dehydration of isopropanol*, Chem. Eng. Sci. 56 (2001) 1419–1427.
- [8] C. de Bellefon, N. Tanchoux, S. Caravieilh, P. Grenouillet, V. Hessel, *Angew. Chem. Int. Ed.* 39 (2000) 3442.
- [9] C. de Bellefon, R. Abdallah, T. Lamouille, N. Pestre, S. Caravieilh, P. Grenouillet, *High throughput screening of molecular catalysts using automated liquid handling, injection and micro-devices*, Chimia 56 (2002) 621–626.
- [10] R. Abdallah, V. Meille, J. Shaw, D. Wenn, C. de Bellefon, *Gas–liquid and gas–liquid–solid catalysis in a mesh micro-reactor*, Chem. Commun. (2004) 372.
- [11] S.K. Ajmera, C. Delattre, M. Schmidt, K.F. Jensen, *Micro-fabricated differential reactor for heterogeneous gas phase catalyst testing*, J. Catal. 209 (2002) 401–412.
- [12] C. de Bellefon, N. Pestre, T. Lamouille, P. Grenouillet, V. Hessel, *Adv. Synth. Catal.* 345 (2003) 190.
- [13] V. Hessel, H. Löwe, A. Müller, G. Kolb, *Chemical Micro-process Engineering: Processing and Plants*, Wiley-VCH, Weinheim, 2005.
- [14] M.G. Pollack, R.B. Fairb, A.D. Shenderov, *Electrowetting-based actuation of liquid droplets for micro-fluidic applications*, Appl. Phys. Lett. 77 (2000) 1725–1726.
- [15] K. Jahnisch, M. Baerns, V. Hessel, W. Ehrfeld, V. Haverkamp, H. Lowe, Ch. Wille, A. Guber, *J. Fluorine Chem.* 105 (2000) 117.
- [16] *Micro-bubble Beam (MBB), A potential dispersion mechanism for multi-phase gas–liquid micro-reactor systems* Doku George N, *Ind. Eng. Chem. Res.* 42 (2003) 3721–3730.
- [17] S. Hardt, T. Dietrich, A. Freitag, V. Hessel, H. Löwe, C. Hofmann, A. Oroskar, F. Schönfeld, K. Vanden Bussche, *Radial and tangential injection of liquid/liquid and gas/liquid streams and focusing thereof in a special cyclone mixer*, in: *Proceedings of the Sixth International Conference on Micro-reaction Technology, IMRET 6 AICHE Pub. No. 164: New Orleans, USA, 2002, 2002*, pp. 329–344.
- [18] (a) N. de Mas, A. Guenther, M.A. Schmidt, K.F. Jensen, *Micro-fabricated multiphase reactors for the selective direct fluorination of aromatics*, *Ind. Eng. Chem. Res.* 42 (2003) 698;  
(b) M.W. Losey, M.A. Schmidt, K.F. Jensen, *Micro-fabricated multiphase packed-bed reactors: characterization of mass transfer and reactions*, *Ind. Eng. Chem. Res.* 40 (2001) 2555.
- [19] J. Kobayashi, Y. Mori, K. Okamoto, R. Akiyama, M. Ueno, T. Kitamori, S. Kobayashi, *A micro-fluidic device for conducting gas–liquid–solid hydrogenation reactions*, *Science* 304 (2004) 1305–1308.
- [20] K.-K. Yeong, A. Gavrilidis, R. Zapf, V. Hessel, *Catalyst preparation and deactivation issues for nitrobenzene hydrogenation in a micro-structured falling film reactor*, *Catal. Today* 81 (2003) 641.
- [21] R.D. Chambers, D. Holling, A.J. Rees, G. Sandford, *Micro-reactors for oxidations using fluorine*, *J. Fluorine Chem.* 119 (2003) 81–82 (and references cited therein).
- [22] (a) E.N. Jacobsen, A. Pfaltz, H. Yamamoto (Eds.), *Handbook of Asymmetric Catalysis*, Springer, 2000 (many examples can be found);  
(b) R. Noyori, *Asymmetric Catalysis in Organic Synthesis*, Wiley, New York, 1994.
- [23] V. Meille, N. Pestre, P. Fongarland, C. de Bellefon, *Gas–liquid mass transfer in small laboratory batch reactors: comparison of methods*, *Ind. Chem. Eng. Res.* 43 (2004) 924–927.
- [24] N. Pestre, PhD thesis, Université Claude Bernard de Lyon, 2004.